View metadata, citation and similar papers at core.ac.uk

brought to you by CORE

provided by Chalmers Publication Library

CHALMERS

Chalmers Publication Library

Experimental analysis of degenerate vector phase-sensitive amplification

This document has been downloaded from Chalmers Publication Library (CPL). It is the author´s version of a work that was accepted for publication in:

Optics Express (ISSN: 1094-4087)

Citation for the published paper:
Lorences Riesgo, A. ; Chiarello, F. ; Lundström, C. (2014) "Experimental analysis of degenerate vector phase-sensitive amplification". Optics Express, vol. 22(18), pp. 21889-21902.

http://dx.doi.org/10.1364/OE.22.021889

Downloaded from: http://publications.lib.chalmers.se/publication/202431

Notice: Changes introduced as a result of publishing processes such as copy-editing and formatting may not be reflected in this document. For a definitive version of this work, please refer to the published source. Please note that access to the published version might require a subscription.

Chalmers Publication Library (CPL) offers the possibility of retrieving research publications produced at Chalmers University of Technology. It covers all types of publications: articles, dissertations, licentiate theses, masters theses, conference papers, reports etc. Since 2006 it is the official tool for Chalmers official publication statistics. To ensure that Chalmers research results are disseminated as widely as possible, an Open Access Policy has been adopted.
The CPL service is administrated and maintained by Chalmers Library.

(article starts on next page)

Experimental analysis of degenerate vector phase-sensitive amplification

Abel Lorences-Riesgo,[1,*] Fabrizio Chiarello,[2] Carl Lundström,[1] Magnus Karlsson,[1] and Peter A. Andrekson[1]

[1] *Photonics Laboratory, Department of Michrotechnology and Nanoscience (MC2), Chalmers University of Technology, Gothenburg, SE412-96, Sweden*
[2] *Department of Information Engineering, University of Padova, Via G. Gradenigo 6/B, Padova, 35131, Italy*

[*] *lorences@chalmers.se*

Abstract: We comprehensively investigate a degenerate vector phase-sensitive amplifier (PSA). We determine the gain dependence on the relative phase and polarization angle between the pumps and the degenerate signal wave. The vector PSA is experimentally shown to be sensitive to the pump states of polarization (SOP) due to polarization mode dispersion in the fiber. However, the scheme performance agrees well with theory under specific pump SOPs and we achieve an on-off gain over 10 dB with a small deviation from the theoretically expected results. In comparison to the scalar scheme, the proposed vector scheme has larger tolerance for pump depletion due to four-wave mixing between pumps and generation of higher-order idlers.

© 2014 Optical Society of America

OCIS codes: (060.2320) Fiber optics amplifiers and oscillators; (190.4970) Parametric oscillators and amplifiers; (190.4380) Nonlinear optics, four-wave mixing.

References and links

1. C. M. Caves, "Quantum limits on noise in linear amplifiers," Phys. Rev. D **26**, 1817–1839 (1982).
2. K. Croussore, I. Kim, C. Kim, Y. Han, and G. Li, "Phase-and-amplitude regeneration of differential phase-shift keyed signals using a phase-sensitive amplifier," Opt. Express **14**, 2085–2094 (2006).
3. R. Slavík, F. Parmigiani, J. Kakande, C. Lundström, M. Sjödin, P. A. Andrekson, R. Weerasuriya, S. Sygletos, A. D. Ellis, and L. Grüner-Nielsen, "All-optical phase and amplitude regenerator for next-generation telecommunications systems," Nat. Photonics **4**, 690–695 (2010).
4. J. A. Levenson, I. Abram, T. Rivera, and P. Grangier, "Reduction of quantum noise in optical parametric amplification," J. Opt. Soc. Am. B **10**, 2233–2238 (1993).
5. K. J. Lee, F. Parmigiani, S. Liu, J. Kakande, P. Petropoulos, K. Gallo, and D. Richardson, "Phase sensitive amplification based on quadratic cascading in a periodically poled lithium niobate waveguide," Opt. Express **17**, 20393–20400 (2009).
6. T. Umeki, O. Tadanaga, A. Takada, and M. Asobe, "Phase sensitive degenerate parametric amplification using directly-bonded PPLN ridge waveguides," Opt. Express **19**, 6326–6332 (2011).
7. Z. Tong, C. Lundström, P. A. Andrekson, C. J. McKinstrie, M. Karlsson, D. J. Blessing, E. Tipsuwannakul, B. J. Puttnam, H. Toda, and L. Grüner-Nielsen, "Towards ultrasensitive optical links enabled by low-noise phase-sensitive amplifiers," Nat. Photonics **5**, 430–436 (2011).
8. C. McKinstrie and S. Radic, "Phase-sensitive amplification in a fiber," Opt. Express **12**, 4973–4979 (2004).
9. C. McKinstrie, M. Raymer, S. Radic, and M. Vasilyev, "Quantum mechanics of phase-sensitive amplification in a fiber," Opt. Commun. **257**, 146–163 (2006).
10. C. J. McKinstrie, S. Radic, M. G. Raymer, and L. Schenato, "Unimpaired phase-sensitive amplification by vector four-wave mixing near the zero-dispersion frequency," Opt. Express **15**, 2178–2189 (2007).
11. M. E. Marhic, "Polarization independence and phase-sensitive parametric amplification," J. Opt. Soc. Am. B **28**, 2685–2689 (2011).
12. R. Jopson and R. Tench, "Polarisation-independent phase conjugation of lightwave signals," Electron. Lett. **29**, 2216–2217 (1993).

#212858 - $15.00 USD Received 27 May 2014; revised 15 Aug 2014; accepted 20 Aug 2014; published 2 Sep 2014

13. K. Inoue, "Polarization independent wavelength conversion using fiber four-wave mixing with two orthogonal pump lights of different frequencies," J. Lightwave Technol. **12**, 1916–1920 (1994).
14. K.-Y. Wong, M. Marhic, K. Uesaka, and L. G. Kazovsky, "Polarization-independent two-pump fiber optical parametric amplifier," IEEE Photon. Technol. Lett. **14**, 911–913 (2002).
15. S. Radic and C. McKinstrie, "Two-pump fiber parametric amplifiers," Opt. Fiber Technol. **9**, 7–23 (2003).
16. A. Lorences Riesgo, C. Lundström, M. Karlsson, and P. Andrekson, "Demonstration of degenerate vector phase-sensitive amplification," in "39th European Conference and Exhibition on Optical Communication (ECOC 2013), paper We.3.A.3," (2013).
17. G. Agrawal, *Nonlinear Fiber Optics*, Optics and Photonics (Elsevier Science, 2013), 5th ed.
18. C. J. McKinstrie and M. G. Raymer, "Four-wave-mixing cascades near the zero-dispersion frequency," Opt. Express **14**, 9600–9610 (2006).
19. F. Yaman, Q. Lin, and G. Agrawal, "Effects of polarization-mode dispersion in dual-pump fiber-optic parametric amplifiers," IEEE Photon. Technol. Lett. **16**, 431–433 (2004).
20. X. Liu, A. R. Chraplyvy, P. J. Winzer, R. W. Tkach, and S. Chandrasekhar, "Phase-conjugated twin waves for communication beyond the kerr nonlinearity limit," Nat. Photonics **7**, 560–568 (2013).
21. J. Kakande, C. Lundström, P. A. Andrekson, Z. Tong, M. Karlsson, P. Petropoulos, F. Parmigiani, and D. J. Richardson, "Detailed characterization of a fiber-optic parametric amplifier in phase-sensitive and phase-insensitive operation," Opt. Express **18**, 4130–4137 (2010).
22. M. Gao, T. Inoue, T. Kurosu, and S. Namiki, "Evolution of the gain extinction ratio in dual-pump phase sensitive amplification," Opt. Lett. **37**, 1439–1441 (2012).

1. Introduction

A phase-sensitive amplifier (PSA) amplifies the in-phase quadrature of a signal wave with a quantum-limited noise figure (NF) of 0 dB [1] while attenuating the out-of-phase quadrature. Thus, PSAs are capable of noiseless amplification. This contrasts with the 3 dB quantum-limited NF of phase-insensitive amplifiers (PIAs), such as commercially available erbium-doped fiber amplifiers (EDFAs) which amplify both quadratures equally. Moreover, since PSAs amplify only the in-phase component, they can provide phase squeezing in e.g. all-optical regeneration of phase encoded signals [2, 3].

PSAs can be realized in χ^2 [4–6] and χ^3 [3, 7] nonlinear materials. In both types of materials, investigations have covered degenerate (signal and idler at the same frequency) [3, 6] and non-degenerate (signal and idler at different frequencies) [5, 7] schemes. However, demonstrations have mainly been performed with scalar schemes in which all interacting waves are co-polarized. Theoretical studies have also covered vector schemes where the pumps are cross-polarized [8–11]. Vector schemes are quite attractive for phase-insensitive fiber-optic parametric amplifiers (PI-FOPAs) since they can provide polarization-insensitive wavelength conversion and amplification without the use of polarization diversity [12–15]. This polarization-insensitive amplification comes at the expense of lower gain compared to the scalar PI-FOPA scheme.

In contrast to the vector PI-FOPA scheme which has been thoroughly investigated, not so much attention has previously been given to the vector PS schemes. We recently demonstrated a degenerate vector phase-sensitive (PS)-FOPA scheme with an on-off gain of about 5 dB [16]. Although the scheme was shown to be polarization-sensitive, the potential of using vector PS schemes for amplification or signal processing of polarization-division multiplexing (PDM) data is quite attractive since they are less complex than polarization-diversity scalar schemes which are not polarization-insensitive [11]. Therefore, an analysis of the performance and limitations on vector schemes is necessary in order to understand the capabilities of vector schemes as amplifiers and regenerators of PDM data signals.

In this paper, we extend the work presented in [16]. We comprehensively analyze theoretically as well as experimentally a degenerate vector PSA. We analytically evaluate the gain dependence on the relative polarization and phase between the input waves. Based on the theoretical expressions, we comment on some potential applications of the degenerate vector PSA. Experimentally, we also characterize the gain of a degenerate vector PSA as a function of

#212858 - $15.00 USD Received 27 May 2014; revised 15 Aug 2014; accepted 20 Aug 2014; published 2 Sep 2014
(C) 2014 OSA

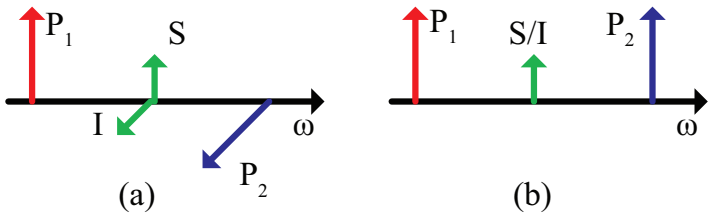

Fig. 1. (a): Polarization diagram for the degenerate vector PSA. (b): Polarization diagram for the degenerate scalar PSA. P_1 pump at lowest frequency, P_2 pump at highest frequency; S, signal; I, idler. Note that any axis polarization rotation can be applied over both diagrams schemes without losing validity as long as the indicated orthogonality relation between the signal, idler and pump polarizations are maintained. In other words, the pump, signal and idler are do not need to be linearly polarized.

the relative phase and polarization. Our experiments cover the analysis on the effects from polarization-mode dispersion (PMD), showing that the scheme is quite sensitive to PMD perturbations. Fiber PMD can make the experimental results deviate from the predicted results in which we neglected such effects. However, good agreement between the theoretical predictions and the experimental results is achieved for specific states of polarization (SOPs) of the pumps. We experimentally demonstrate, to the best of our knowledge, the first vector PSA with a large net gain ($\sim$10 dB). Additionally, we compare the proposed scheme with the conventional degenerate scalar PSA. Unlike the vector PSA scheme, the scalar scheme is strongly affected by the presence of higher order idler and pump depletion due to four-wave mixing (FWM) between the pumps.

2. Theoretical description

2.1. Vector scheme, gain dependence on the relative polarization angle and phase

The configuration for the degenerate vector PSA is shown in Fig. 1(a) where two pumps, P_1 and P_2, at frequencies ω_1 and ω_2 are cross-polarized. PS interaction occurs between the signal, S, and idler, I, which are the two orthogonal components (projected over the pump polarizations) of the wave referred along this paper as the degenerate wave with frequency $\omega_S = \omega_I = (\omega_{P1} + \omega_{P2})/2$. The output fields as a function of the input fields can be described by [8]

$$S_{out} = \mu_V S_{in} + \nu_V I_{in}^* \tag{1}$$

$$I_{out} = \mu_V I_{in} + \nu_V S_{in}^*, \tag{2}$$

where the coefficients μ_V and ν_V are the coefficients of the matrix transformation for the vector scheme and fulfill $|\mu_V|^2 - |\nu_V|^2 = 1$. Assuming that the phase matching condition is fulfilled, a fiber with random birefringence and equal pump powers, P, then $\mu_V = \cosh(\gamma PL)$ where γ is the nonlinear coefficient of the fiber and L is the fiber length.

The polarization diagram of this scheme is represented in Fig. 2. The pump polarizations are antipodal on the Poincaré sphere. In our example, the pumps are circularly polarized but they can take any polarization as long as they are orthogonal. The degenerate wave polarization forms an angle α (defined in the Stokes space) with P_1. The azimuth of the degenerate wave, Ψ, defines the phase difference between the signal and idler (components of the degenerate wave projected over the pump polarization). With these definitions, the power gain for the degenerate wave can be then determined as

$$G_V = |\mu_V|^2 + |\nu_V|^2 + 2|\mu_V||\nu_V|\sin(\alpha)\cos(\phi), \tag{3}$$

#212858 - $15.00 USD Received 27 May 2014; revised 15 Aug 2014; accepted 20 Aug 2014; published 2 Sep 2014
(C) 2014 OSA

where $\phi = \phi_{P_1,in} + \phi_{P_2,in} - \phi_{S_{in}} - \phi_{I_{in}}$ is the relative phase difference between the pumps, the signal and the idler.

Equation (3) shows that the SOP of the degenerate wave determines whether the amplifier is working in PS or PI mode. PI operation can be achieved when the degenerate wave is co-polarized with one of the pumps, $\alpha = 0^\circ$ or $\alpha = 180^\circ$. Under any other SOP of the degenerate wave, the amplifier is working in PS mode. The PS interaction is maximized when the signal and idler have the same power. Therefore, maximum PS interaction occurs when the degenerate wave forms a 90° angle with the pumps.

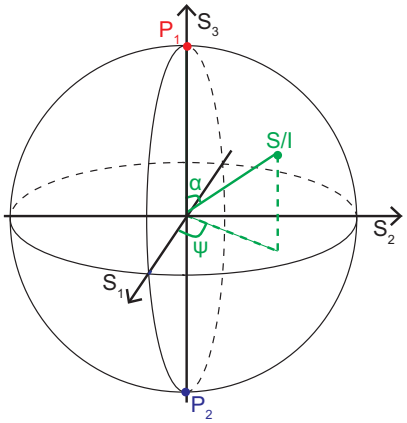

Fig. 2. Diagram of the degenerate vector PSA on the Poincaré sphere. S_1, S_2 and S_3 correspond to the Stokes axis. P_1, P_2 indicates the pump polarizations. S/I shows the polarization of the degenerate wave formed by the signal and idler.

2.2. *Scalar scheme, gain dependence on the relative polarization angle and phase*

The conventional scalar degenerate PSA consists of two pumps and signal/idler all with the same polarization as depicted in Fig. 1(b). The relation between the output and input can be the expressed as [8]

$$S_{out} = \mu_S S_{in} + \nu_S S_{in}^*, \tag{4}$$

where μ_S and ν_S are the coefficients of the matrix transformation for the scalar scheme which also fulfills $|\mu_S|^2 - |\nu_S|^2 = 1$. In this case, $\mu_S = \cosh(2\gamma PL)$ when again assuming perfect phase matching and equal pump powers, P. Therefore, compared to the vector case, μ_S takes an amplitude value that is the double in dBs of μ_V in the high gain regime.

If we consider a degenerate wave, a wave with frequency ω_S but with an arbitrary SOP, with polarization angle, α, with respect to the pumps, the gain can be determined by [17]

$$G_S = \left(|\mu_S|^2 + |\nu_S|^2 + 2|\mu_S||\nu_S|\cos(\phi)\right)\cos^2(\alpha/2) + \sin^2(\alpha/2), \tag{5}$$

where the Manakov model is assumed and higher-order FWM processes such as Bragg-scattering wavelength conversion are neglected. In this case, the relative phase is defined as $\phi = \phi_{P_1,in} + \phi_{P_2,in} - 2\phi_{P_s,in}$.

2.3. *Additional effects: higher-order idlers and PMD*

The previous equations are valid for the case where only three waves at three different wavelengths are involved. However, higher-order idlers, waves at frequencies $\omega_{HOI1} = 2\omega_{P1} - \omega_S$

#212858 - $15.00 USD Received 27 May 2014; revised 15 Aug 2014; accepted 20 Aug 2014; published 2 Sep 2014
(C) 2014 OSA

and $\omega_{HOI2} = 2\omega_{P2} - \omega_S$, are created by the modulation instability and Brag Scattering processes. The equations previously presented assumes such higher-order idlers are negligible. The influence of higher order idler has been studied previously for both scalar [18] and vector [10] PSA schemes when both schemes are operating near the zero dispersion wavelength. These studies showed that the scalar PSA is more affected by the higher-order idlers than the vector PSA.

PMD effects have also been neglected in the derivation for the aforementioned equations. PMD effects have been studied extensively for vector PI-FOPA [19] in which PMD induces polarization-dependent gain. In the degenerate vector PSA scheme, PMD manifests as a dependence of the signal gain on the azimuth angle, Ψ. With random birefringence, the pump orthogonality is not maintained along the fiber. Small misalignments between the pumps create an azimuth-dependent gain. However, in our experiments we tried to suppress theses effects by optimizing the pump SOPs launched into the fiber.

2.4. Applications of a degenerate vector PSA

A non-degenerate PSA can amplify data independently of the modulation format as long as the idler is a conjugated copy of the signal [7]. The degenerate vector PSA can also amplify modulation-independent data with the same condition, the idler is a conjugated copy of the signal where signal and idler are two waves with the same frequency but orthogonal polarizations as shown in Fig. 1(a). For example, if we modulate two conjugated copies of a quadrature phase-shift keying (QPSK) signal in the signal and idler, they are amplified by the PSA. The two conjugated copies of the QPSK signal modulated on two orthogonal polarizations are equivalent to PDM-binary phase-shift keying (PDM-BPSK). Therefore, the proposed scheme can PS amplify a PDM-BPSK signal with a proper polarization alignment in which we can express the PDM-BPSK signal as two conjugated QPSK signals and each one of the QPSK signals is co-polarized with each pump. Therefore, a PDM-BPSK signal can be PS-amplified or phase regenerated without the need of polarization diversity schemes which increase the system complexity.

In connection to PS amplification of PDM-BPSK signals, we can observe that a degenerate vector PSA can also perform format conversion from a single-polarization QPSK signal to a PDM-BPSK signal. In order to perform QPSK to PDM-BPSK conversion, the scheme should PI amplify the QPSK which means that only signal or idler are present at the input. Assuming high gain and no input idler, from Eqs. (1), (2) we can observe that the degenerate vector PSA creates a conjugated copier of the QPSK signal on the idler. The two conjugated QPSK signals on orthogonal polarizations and same frequency are equivalent to a PDM-BPSK signal. Readers should realize that a similar scheme with two conjugated QPSK signals on orthogonal polarizations has been demonstrated in order to compensate distortion due to fiber nonlinearities [20].

In addition, in a more general way, a vector PSA has potential for phase-to-polarization conversion when assuming high gain and PI operation. With no input idler and high gain, both output signal and idler will have about the same power in accordance with Eqs. (1), (2) and the output idler will be a conjugated copier of the signal. This means that the output degenerate wave is formed by two conjugated copies on two orthogonal polarization. Therefore, its polarization is determined by the phase relation between the output idler and signal which in turn is determined by the input signal phase.

#212858 - $15.00 USD Received 27 May 2014; revised 15 Aug 2014; accepted 20 Aug 2014; published 2 Sep 2014
(C) 2014 OSA

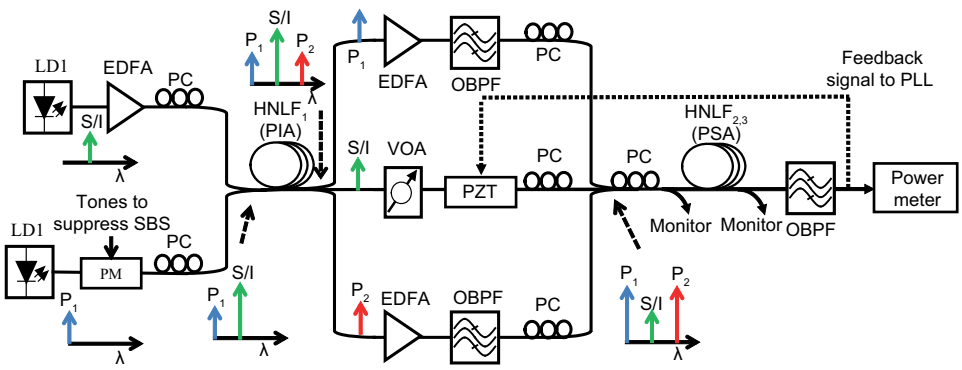

Fig. 3. Experimental setup. Pumps (P_1 and P_2), signal (S) and idler (I) are defined for the PSA. LD, laser diode; EDFA, erbium-doped fiber amplifier; PC, polarization controller, PM, phase modulator; HNLF, highly-nonlinear fiber; PIA, phase-insensitive amplifier; OBPF, optical band-pass filter; VOA, variable optical attenuator; PZT, piezoelectric transducer; PSA, phase-sensitive amplifier; PLL, phase-locked loop.

3. Experiment

3.1. Setup

The experimental setup is shown in Fig. 3. Two tunable laser diodes (LDs) generate two waves at wavelengths of $\lambda_1 = 1558.5\ nm$ and $\lambda_s = 1571\ nm$. The wave at λ_1 was phase modulated in order to avoid stimulated Brillouin scattering (SBS) in the PSA stage. The wave at 1571 nm was amplified by a high-power EDFA. Out of band amplified-spontaneous emission (ASE) noise was removed with an optical band-pass filter (OBPF). Both waves were combined by a wavelength-division multiplexing (WDM) coupler before being injected into a PIA stage, the so-called copier [7], with aligned polarizations. Before the PIA, the power of the wave at 1558.5 nm, which acted as the signal in the copier stage, was about 12 dBm. The wave at 1571 nm acted as the pump in the PIA and its power was about 28 dBm. The copier consisted of a highly-nonlinear fiber (HNLF), $HNLF_1$, which is a aluminium-doped 190 m long fiber with a higher SBS threshold which allowed us to avoid phase modulation on the copier pump. In this copier stage, a third wave at $\lambda_2 = 1584.5$ nm was created with a conversion efficiency of about -10 dB. The three waves are phase locked as required for the proposed scheme.

After the copier, the three waves were split into three different paths. The waves at shortest, P_1, and longest wavelength, P_2, are the pumps for the degenerate PSA. They were both amplified by a C-band and a L-band EDFA. The copier pump acted as signal/idler, S/I, for the degenerate PSA (either vector or scalar). In this path, we placed a piezoelectric transducer (PZT) to stabilize the relative phase between the three waves which was drifting slowly since they were travelling in three different paths. We controlled the SOP of each individual wave by placing a PC in each branch so we could choose between the scalar and the vector scheme. In addition, another PC before the PSA enabled us to rotate the SOP of the three waves simultaneously such that we could evaluate the performance dependence on the pump SOP. The two pumps and the signal/idler were combined before the PS-FOPA. We compared the results of using two different HNLFs, $HNLF_2$ and $HNLF_3$, to implement the PSA. $HNLF_2$ was 125 m long and $HNLF_3$ was 250 m long. Other parameters such as the effective area (A_{eff} 10.1 μm^2), attenuation ($\sim 0.82\ dB/km$), zero dispersion wavelength ($\sim 1569.5\ nm$), third-order dispersion ($\sim 0.026\ ps/(nm^2 km)$) and PMD ($\sim 0.04\ ps/\sqrt{km}$) are quite similar in both fibers since they were cut from the same drawn spool. Before the PSA, we included a monitor port in order to

#212858 - $15.00 USD Received 27 May 2014; revised 15 Aug 2014; accepted 20 Aug 2014; published 2 Sep 2014
(C) 2014 OSA

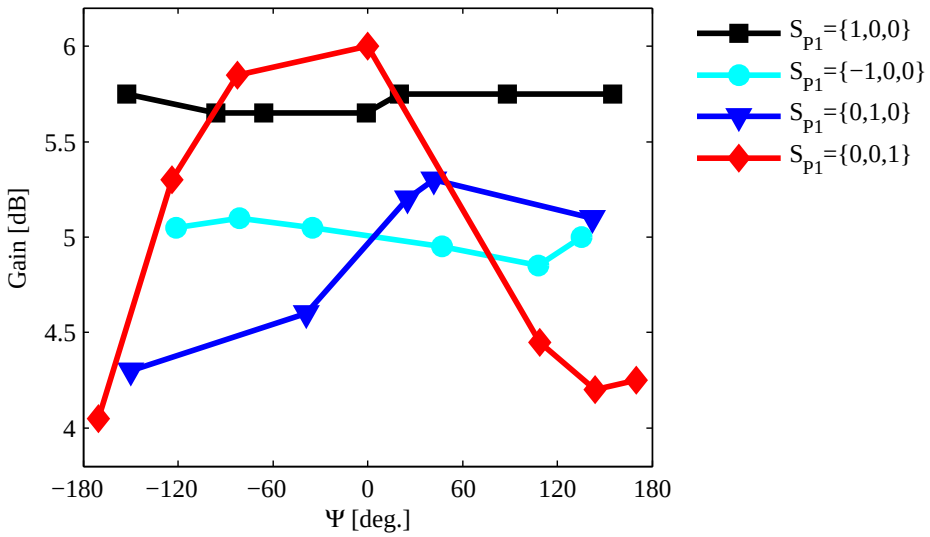

Fig. 4. On-off gain vs. signal azimuth, Ψ, for four different SOPs of the pumps. The legend indicates the Stokes parameters of P_1 with P_2 being orthogonal to P_1. The polarization angle between the degenerate wave and the pumps, α, is about 90° in all cases.

track the relative polarization angle between the waves with a polarimeter and measure the input power of each wave. The polarimeter was placed after an optical processor which allowed us to select the wave into the polarimeter. After the PSA, we also monitor the output power and SOP. Then, the degenerate wave was filtered and monitored by an optical power meter. This power meter enabled us to record the signal power (sampling rate of 2048 Hz). Then, we could measure how much the power of the degenerate wave varied due to different relative phases between the waves at the input. Moreover, the degenerate wave was also tapped to a feedback PLL circuit which locked the relative phase between pumps and degenerate wave in order to achieve maximum power on the degenerate wave at the PSA output.

3.2. Results

Using $HNLF_2$, we first evaluated how the gain depended on the azimuth angle, Ψ, which was previously defined in Fig. 2. According to Eq. (3), the gain should not depend on Ψ but due to the fiber PMD this condition is not trivial to achieve experimentally. In order to minimize the dependence on errors measuring the polarization angle, α, these measurements were performed with α values of about 90°. Then, the possible signal SOPs form a circle on the Poincaré sphere. For these measurements, the pump power were about 29 dBm each. Figure 4 shows the signal gain vs. azimuth angle for four different cases of the pump SOPs. When P_1 was aligned close to the Stokes axis S_1, at the input of the polarimeter (square symbols in Fig. 4) the dependence of the signal gain on the azimuth was of about 0.3 dB. When we inverted the pump polarization with respect to the previous case (circle symbols in Fig. 4) the gain was lowered by about 0.7 dB but it still did not have large fluctuation with regard to the azimuth, Ψ. It was confided within a range lower than 0.3 dB. In these two measurements, the output degree of polarization (DOP) was about 8% where $DOP = |<\overline{S}>|/<|\overline{S}|>$, $\overline{S}$ is the Stokes vector of the full optical field, $|S|$ is the total optical power and $<x>$ denotes long-term (ms, given by polarimeter response time) average. In our case the optical field is dominated by the pumps, which are incoherent with each other, making $<\overline{S}>$ the sum of the pumps Stokes

#212858 - $15.00 USD Received 27 May 2014; revised 15 Aug 2014; accepted 20 Aug 2014; published 2 Sep 2014
(C) 2014 OSA

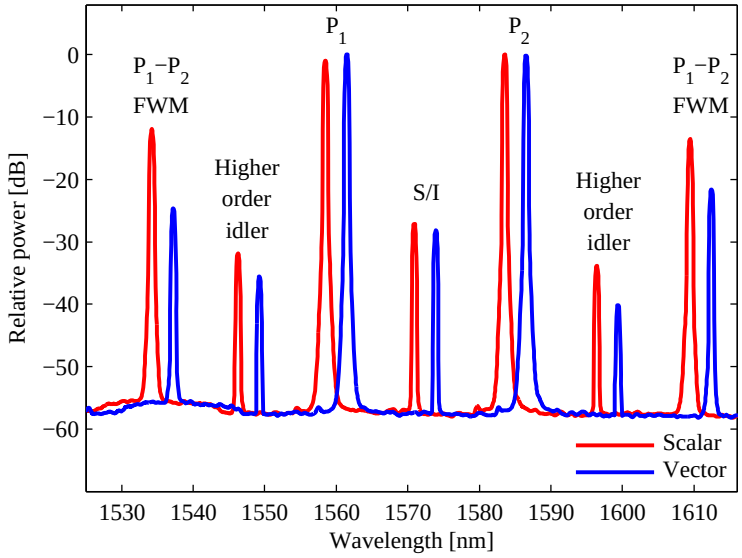

Fig. 5. Measured output spectra for the vector ($\alpha = 90°$) and scalar ($\alpha = 0°$) cases with maximum signal amplification using $HNLF_2$. The vector spectrum was shifted 3 nm for clarity.

vectors. When the pumps are equal in power which is the case in our experiment since pump powers are equalized in the optical processor before the polarimeter, $< \bar{S} >$ is close to zero for orthogonal pumps. We also studied another two cases, P_1 with linear polarization of +45° (triangles) and with right circular polarization (diamonds). In these two cases, the gain had variation larger than 1 dB when modifying the azimuth angle. The output DOP was about 13% when P_1 had linear polarization of +45° and about 14% when P_1 polarization corresponded to right circular polarization. Then, even though we are using a short-fiber with low gain, the degenerate vector PSA is quite sensitive to PMD since the orthogonality between the pumps were broken. However, it seems that under optimized pump SOPs the azimuthal dependence can be negligible. These specific pump SOPs seems to be the principal states of polarization of the HNLF since they approximately maintain pump orthogonality.

Once we have demonstrated that we can minimize the azimuth dependence, we decided to increase the pump powers to 29.5 dBm each (maximum available) and maximize the gain. Fig. 5 shows the output spectra for the vector and scalar PSA with a signal power of about -7 dBm at the PSA input. In the vector PSA, we optimized the pump SOPs in order to minimize the azimuth dependence when $\alpha = 90°$. The output vector spectrum was taken when the polarization angle, α, was about 90°. With this polarization angle, the on-off gain about 6 dB. The scalar output spectrum is shown for the case with the degenerate wave was aligned to the pumps, $\alpha = 0°$, for which we achieved the maximum scalar gain, about 8 dB. In both cases, apart from amplifying the degenerate wave the PSA created additional signal corresponding to higher-order idlers and FWM terms between the pumps. As expected, higher-order idlers and pump FWM terms were stronger for the scalar PSA than for the vector PSA.

With these conditions, we assessed the gain as a function of the polarization angle, α, between the degenerate wave and P_1 for the vector and the scalar schemes as shown in Fig. 6. The theoretical curves are based on the Eqs. 3, 5 with only the maximum gain as fitting parameter. We also include simulation results where we simulated both schemes by applying the

#212858 - $15.00 USD Received 27 May 2014; revised 15 Aug 2014; accepted 20 Aug 2014; published 2 Sep 2014
(C) 2014 OSA

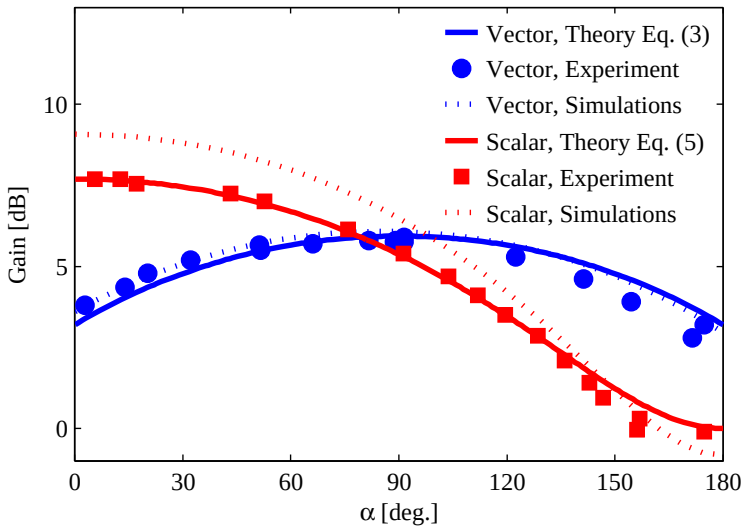

Fig. 6. On-off gain vs. polarization angle, α, using $HNLF_2$ for the vector (blue) and scalar (red) schemes with the polarization angle defined in Stokes space. The solid lines represent the theoretical curves, dotted line represent simulation results and the symbols represent measured data.

split-step Fourier method to the Manakov equation in order to clarify disagreement between the theory and the experimental data. The parameters which we used to model the fiber and the pump powers are the aforementioned ones, with the only fitting parameter being the nonlinear coefficient of the fiber, $\gamma = 10.5\ (W\ km)^{-1}$ when simulating $HNLF_2$ and $\gamma = 12.5\ 1\ (W\ km)^{-1}$ when simulating $HNLF_3$. Note that PMD effects were neglected in our simulations.

In these measurements, we stabilized the signal output by activating the PLL circuit. In the vector PSA, we measured different degenerate wave SOPs for the maximum PS interaction, $\alpha = 90^\circ$, with different azimuths and in all the cases the gain was about 6 dB. The minimum gain, about 3 dB, was obtained when the signal polarization was aligned to P_2. When the signal polarization was parallel to P_1, the gain was about 3.8 dB which shows that the experimental gain was slightly asymmetric with an about 0.8 dB larger gain when the signal was aligned to P_1 ($\alpha = 0^\circ$) than when it was aligned to P_2 ($\alpha = 180^\circ$). Our simulations confirmed that this asymmetry is mainly due to the modulation instability process since the experimental results fit quite well the simulation results. Apart from the asymmetry, the measurements also follow the theoretical curve showing the expected polarization gain dependence. In the scalar scheme, as said, the maximum achieved gain, about 8 dB, was achieved with aligned polarizations between the degenerate wave and the pumps. The experimental results also fit quite well the predicted results by the theory. Maximum gain is achieved when the degenerate wave is aligned with the pumps. When the degenerate wave is orthogonal to the pumps, the gain vanishes. The simulations results are also close to the experimental results although the simulations predicted slightly higher gain which can be due to slightly wrong modelling of the fiber.

Figure 7 shows the power swing (maximum gain / maximum attenuation) of the degenerate wave at the output when not stabilizing the phases of the waves. In these measurements, the electrical signal driving the PZT was disconnected. The theoretical swing is calculated using Eqs. (3), 5 using the maximum gain at $\phi = 0^\circ$ and maximum attenuation at $\phi = 180^\circ$. The swing goes from about 0 dB when the signal is parallel to one of the pumps, $\alpha = 0, 180^\circ$, to

#212858 - $15.00 USD Received 27 May 2014; revised 15 Aug 2014; accepted 20 Aug 2014; published 2 Sep 2014
(C) 2014 OSA

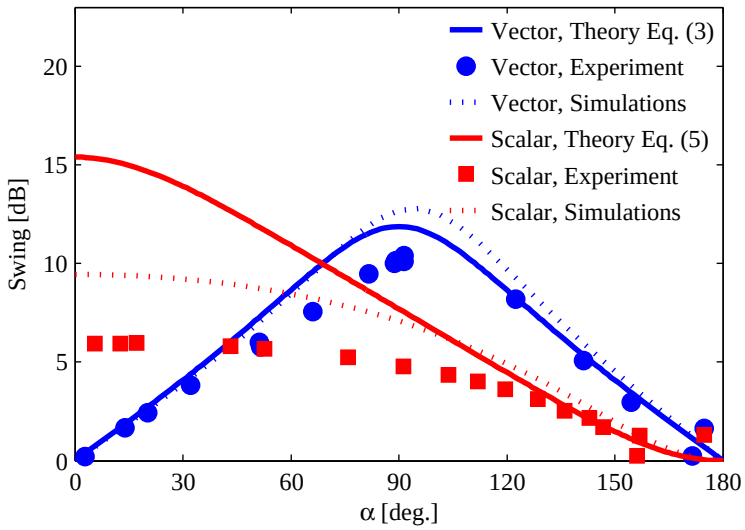

Fig. 7. Degenerate wave power swing (maximum gain/maximum attenuation) vs. polarization angle, α using $HNLF_2$ for the vector (blue) and scalar (red) schemes with the polarization angle defined in Stokes space. The solid lines represent the theoretical curves, dotted line represent simulation results and the symbols represent measured data.

about 11 dB when $\alpha = 90^\circ$. The curve for the swing is quite symmetric. This confirms that the process creating the asymmetry in the gain is phase-insensitive since it does not affect the swing but shifts the gain curve. We did not obtain the same swing as predicted by the theory and simulations. This can be explained by limitations of the measurement method and the pump phase modulation [21]. Both effects limited the maximum attenuation that we could measure. Concerning the scalar case, we see that the swing is quite limited. Indeed, the maximum swing is lower than the maximum gain. This can be explained by the creation of higher-order idlers, see Fig. 5, which limited the attainable attenuation. The theory of the three-wave interaction is not valid in this case. However, our simulations results also predict lower swing than double the gain in dBs.

We then decided to use $HNLF_3$ in order to achieve a higher gain. Each pump power was again 29.5 dBm. Therefore, the main difference with the previous case was the HNLF length, 250 m in $HNLF_3$ and 125 m in $HNLF_2$. The signal power was about -7 dBm for the vector scheme and about -14 dBm for the scalar case in order to avoid saturation in the scalar PSA. The output spectra for the maximum scalar, $\alpha = 0^\circ$, and vector, $\alpha = 90^\circ$, PS gain is plotted in Fig. 8. In the vector case, the azimuthal dependence was again minimized by aligning the pump SOPs and we achieved a maximum 10.5 dB gain with a polarization angle of about 90°. In the scalar PSA, the maximum gain with $HNLF_3$ was about 23 dB and polarization angle of about 0°. When comparing to the previous vector PSA implemented with $HNLF_2$, the maximum vector gain which has been almost doubled its value in dBs by using $HNLF_3$. In the scalar case, the gain increased from 8 dB to about 23 dB. This increase can be explained by taking into account higher-order idlers and small difference in the fiber parameters. Note that without accounting for higher-order idlers, the gain is doubled in dBs when the fiber length is doubled, any other parameter is constant and assuming perfect phase matching. However, the gain difference between the amplifier using $HLNF_3$ or using $HNLF_2$ in our simulations was similar to the one found experimentally. By also comparing the results from fibers, the creation

#212858 - $15.00 USD Received 27 May 2014; revised 15 Aug 2014; accepted 20 Aug 2014; published 2 Sep 2014
(C) 2014 OSA

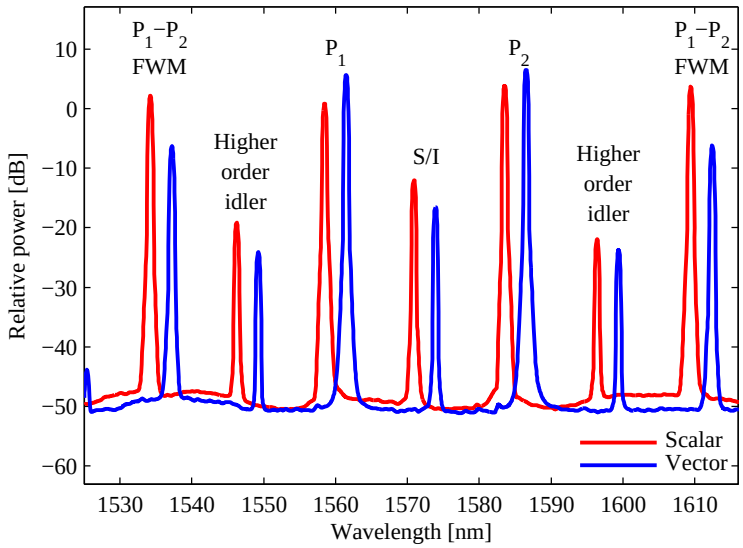

Fig. 8. Measured output spectra for the vector ($\alpha = 90^\circ$) and scalar ($\alpha = 0^\circ$) cases with maximum signal amplification using $HNLF_3$. The vector spectrum was shifted 3 nm for clarity.

of higher-order idlers and terms due to pump FWM was stronger than with $HNLF_2$ in both cases. Again, these created waves were strong in the scalar PSA where pumps were indeed depleted by pump FWM since the waves created by P_1-P_2 FWM have powers of the order of the pump powers.

The gain with regard to the relative polarization angle, α, was again evaluated for both schemes with the conditions for which we took the spectra shown in Fig. 8. As depicted in Fig. 9, analytical and simulation results are quite close. Indeed, the gain curves for the vector PSA are almost indistinguishable when comparing simulations and theory. The experimental results are also close to those predicted by the theory and simulations in both scenarios. In the vector case, we show different measurements with the same polarization angle of $\alpha = 90^\circ$ but different azimuths, Ψ, for which the gain varied within a 0.3 dB range. This shows that even though we have increased the fiber length, which in turn means higher DGD, we can still optimize the pump SOPs and minimize the PMD effects on the gain. The gain when the degenerate wave was aligned to P_1, $\alpha = 0^\circ$, was about 8 dB. When aligning to P_2, $\alpha = 180^\circ$, the gain was about 7.8 dB and the asymmetry was lowered compared to the case of $HNLF_2$. This agrees with the simulation results for which there was negligible asymmetry in the gain curve. The data for the scalar PSA shows that the maximum gain was about 23 dB when both pumps and the degenerate wave were aligned, $\alpha = 0^\circ$. The gain dropped when the degenerate wave polarization was misaligned with respect to the pump polarization. The degenerate wave power was actually the same as without including the pumps when it was orthogonal to the pumps, $\alpha = 180^\circ$. Both the simulations results and the theoretical curve are quite close to the experimental data in the scalar case too.

The power swing vs. polarization angle is depicted in Fig. 10. In the vector scheme, a maximum power swing of about 16 dB occurs when the degenerate wave forms a 90 $^\circ$ angle with both pumps. This power swing is slightly lower than the power swing predicted by either the simulations or theoretically which are both quite close. Again, the phase modulation of the

#212858 - $15.00 USD Received 27 May 2014; revised 15 Aug 2014; accepted 20 Aug 2014; published 2 Sep 2014
(C) 2014 OSA

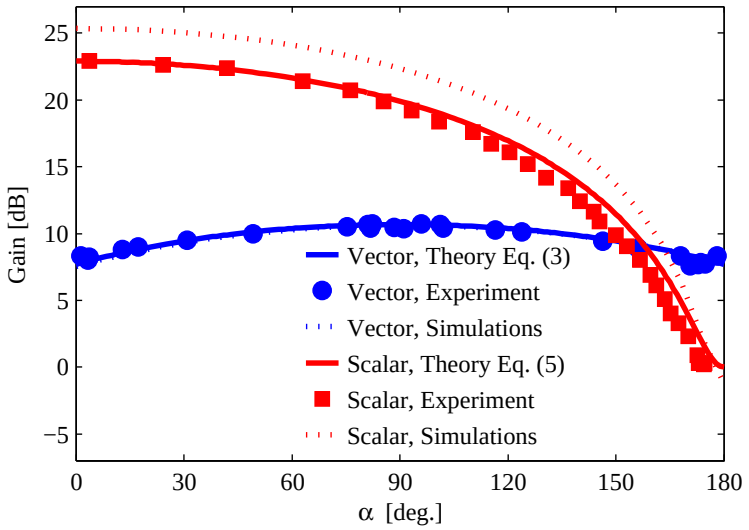

Fig. 9. On-Off gain vs. polarization angle, α, using $HNLF_3$ for the vector (blue) and scalar (red) schemes with the polarization angle defined in Stokes space. The solid lines represent the theoretical curves, dotted line represent simulation results and the symbols represent measured data.

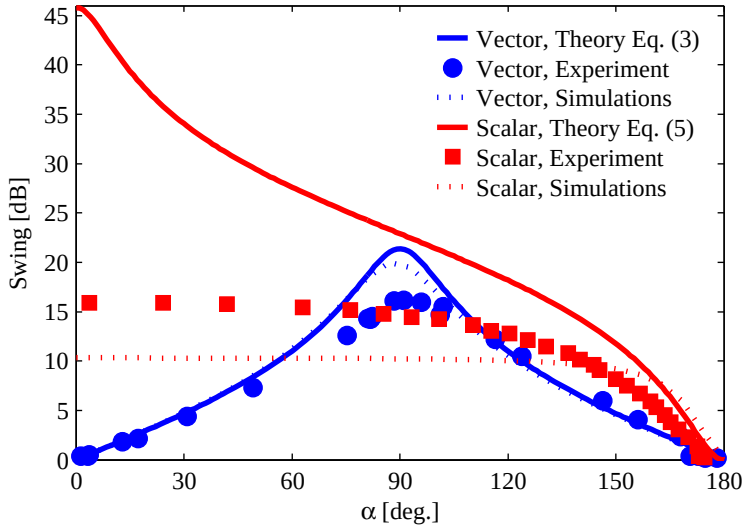

Fig. 10. Degenerate wave power swing (maximum gain/maximum attenuation) vs. polarization angle, α, using $HNLF_3$ for the vector (blue) and scalar (red) schemes with the polarization angle defined in Stokes space. The solid lines represent the theoretical curves, dotted line represent simulation results and the symbols represent measured data.

#212858 - $15.00 USD Received 27 May 2014; revised 15 Aug 2014; accepted 20 Aug 2014; published 2 Sep 2014
(C) 2014 OSA

pumps limited the maximum attenuation. When the degenerate wave is aligned with either of the pumps, the power variation is close to 0 dB. This again confirms that it is acting as a PIA when the degenerate wave polarization is parallel to either of the pump polarizations. The swing for scalar case is quite far from 3-wave-theory prediction. The maximum swing is limited to about 16 dB. This means that the signal is amplified regardless the relative phase between the input waves to the PSA. The simulations of this scenario also predicted a low swing due to the higher-order idlers. Indeed the power swing predicted by the simulation was lower than the power swing measured experimentally which can be explain by some small difference between the modelled fiber parameters and the real fiber. The swing vanished when the degenerate wave was orthogonal, $\alpha = 180^{\circ}$, to the pumps as expected.

3.3. Discussion

The results confirms that a degenerate vector PSA is polarization dependent as predicted by the theory in Section 2. Achieving a polarization independent PSA was already addressed by Marhic [11] which predicted that either degenerate vector PSA or degenerate scalar PSA with polarization diversity are not polarization independent. In our experiments, we got a 2.5 dB gain variation with respect to the polarization angle when optimizing the pump SOP in order to minimize the azimuthal dependence. This gain variation should approximate asymptotically 3 dB when further increasing the gain. Our analysis has not covered the case of a saturated degenerate vector PSA and the gain dependence on the polarization with a saturated vector PSA should be addressed in order to know whether we can minimize the polarization dependence by operating in saturation.

Our experiments also showed that the vector scheme is quite sensitive to fiber PMD. However, we have showed that under specific pump SOP the scheme performance is close to the expected by the theoretical derivations. The PMD in the fiber translates into gain variation for the same polarization angle but different azimuth for the signal. The DGD can be decreased in two ways, using shorter fiber or with small pump wavelength separation. Using shorter fiber translates into lower gain. Reducing the wavelength separation between the pumps also affects the gain. Moreover, the presence of the higher-order idlers is enhanced when decreasing the pump wavelength separation. The higher-order idlers are also affected by PMD. Determining which conditions is less affected by the PMD is quite complex. Nevertheless, pump depletion due to FWM between the pumps is also expected to be weakened when spacing the pumps close in frequency since ideally in the Manakov model there is no pump depletion in the vector scheme [10]. Readers should note that although we have analyzed the degenerate vector PSA, the results regarding PMD effects are quite indicative about such effects on non-degenerate vector PSAs.

In the comparison with the scalar scheme, we have shown that the scalar scheme has larger gain at the same pump power. This higher gain does not translate into larger power swing since the scalar PSA is quite affected by the presence of the higher-order idlers. As previously demonstrated [22], the higher-order idlers can enhance the performance of the scalar scheme by increasing the swing with appropriate dispersion profile and pump wavelength. However, our target was not an optimization of both schemes but a comparison with the same wavelength conditions and pump power. Pump depletion also affects more the scalar PSA when both schemes have the same pump power. Comparing the scalar PSA using $HNLF_2$ to the vector PSA using $HNLF3$ also verifies that the scalar scheme has lower tolerance regarding FWM between pump since the ratio between the pump power and the power of the waves created due to FWM between pumps is $\sim$12 dB in both cases whereas the gain of the vector PSA, 10.5 dB, is 2.5 dB larger than the scalar gain, 8 dB. Thus, the vector PSA has larger gain when the FWM between pumps has the same strength in both schemes.

#212858 - $15.00 USD Received 27 May 2014; revised 15 Aug 2014; accepted 20 Aug 2014; published 2 Sep 2014
(C) 2014 OSA

4. Conclusion

We have theoretically and experimentally analyzed a degenerate vector PSA. We analytically express how the output signal depends on the polarization angle with regard to the pumps and the relative phase. In this derivation, effects from PMD are not included. The theory predicts that maximum PS interaction is achieved when the degenerate wave forms a 90° polarization angle with the pumps. When the degenerate wave is aligned with one of the pumps, the scheme works as a PI system.

Based on the equations which relate the input fields to the output fields, we discussed the potential of the proposed scheme for different applications. The scheme is suitable for PS amplification of PDM-BPSK signals without the need of extra complexity that a polarization diversity scheme would add. Apart from that the scheme can also perform QPSK to PDM-BPSK modulation format conversion and more generally phase to polarization conversion.

Experimentally, we demonstrated the first (to the best of our knowledge) degenerate vector PSA with substantial on-off gain, over 10 dB. The difference between maximum gain and attenuation was about 16 dB. To achieve a large gain we used a HNLF of 250 m length leading to larger PMD effects. We also evaluated the gain when using a HNLF of 125 m. Using this shorter HNLF, the maximum gain was only about 6 dB but suffered less from PMD and higher-order FWM. The scheme is quite sensitive to the SOP of the pumps and small misalignment of the pump polarization makes the gain sensitive to the azimuth angle. However, when the pumps are aligned to these axes, the gain variation with respect to the azimuth is of only about 0.3 dB.

The proposed scheme has been compared with the scalar PSA scheme. The scalar case has larger gain, 8 dB with the 125 m long HNLF and 23 dB with the 250 m long HNLF. However, it also showed higher pump depletion by FWM between the pumps and it is more affected by the presence of higher-order idlers. We have shown that higher-order idlers can limit the PS swing under the operating conditions. Nonetheless, it has been proven that higher-order idlers could also enhance the power swing with other phase matching conditions [22]. In our comparison, we did show that the PS swing could be higher in the vector case than in the scalar case. Therefore, even though one expects higher phase regeneration with the scalar scheme, this is not always the case when we have additional FWM process that cannot be neglected.

Acknowledgments

The research leading to these results received funding from the European Research Council Advanced Grant PSOPA (291618). OFS Denmark and Sumitomo Electric Industries, Ltd. are acknowledged for providing HNLFs. F. Chiarello acknowledges the University of Padova (project “Near Infrared Nonlinear Fiber Oscillators”).

#212858 - $15.00 USD Received 27 May 2014; revised 15 Aug 2014; accepted 20 Aug 2014; published 2 Sep 2014
(C) 2014 OSA